

Coherent Absorption Dynamics: The Dual Role of Off-Diagonal Couplings in Weakly Bound Nuclei

Hao Liu,¹ Jin Lei,^{1,*} and Zhongzhou Ren¹

¹*School of Physics Science and Engineering, Tongji University, Shanghai 200092, China.*

(Dated: January 14, 2026)

Disentangling reaction mechanisms in weakly bound nuclei remains a long-standing challenge, complicated by the common practice of treating absorption as an incoherent sum of channel contributions. Within the Continuum-Discretized Coupled-Channels (CDCC) framework, we derive a generalized coupled-channel optical theorem and show that the total absorption cross section, $\sigma_A \propto -\langle \Psi | W | \Psi \rangle$, decomposes as $\sigma_A = \sigma_D + \sigma_B + \sigma_{\text{int}}$, where σ_{int} is a coherent interference term between channel components. For the systems and complex fragment-target optical potentials considered, σ_{int} is negative and comparable in magnitude to the direct absorption terms. The off-diagonal imaginary couplings play a dual role: they redistribute flux among channels and generate σ_{int} , which is required for flux-balance consistency. In calculations for $d + {}^{93}\text{Nb}$ and ${}^6\text{Li} + {}^{59}\text{Co}/{}^{208}\text{Pb}$, retaining the full non-diagonal coupling matrix nearly doubles the breakup-channel absorption for the heavy target, while reducing the total absorption through σ_{int} . We demonstrate that neglecting the off-diagonal imaginary couplings W_{ij} ($i \neq j$) is not merely an approximation but leads to a *systematically biased physical picture*: the total absorption is overestimated while the breakup absorption component is severely underestimated. Experimental analyses that employ incoherent-sum models to extract direct and breakup cross sections from data will inherit this bias. The full coupling matrix is therefore essential for mechanism-resolved cross-section extraction, and we advocate that experimentalists adopt full-coupling CDCC calculations as the standard for consistent interpretation of absorption data in weakly bound systems.

I. INTRODUCTION

Reactions involving weakly bound nuclei are of fundamental importance in nuclear astrophysics and fusion energy research, where the complex interplay between breakup and fusion processes significantly influences reaction yields [1–9]. A central challenge in modeling these systems is the accurate disentanglement of complete fusion from other reaction channels, and the separation of absorption into direct and breakup components. Addressing this requires a theoretical framework that goes beyond evaluating total reaction probabilities to rigorously separating the absorption cross section into its constituent physical components. By adopting such a component analysis perspective, it becomes possible to explicitly examine how quantum flux is partitioned among distinct pathways and to elucidate the microscopic dynamics governing the transition from the elastic channel and continuum states to the fusion compound.

For these weakly bound systems, the Continuum-Discretized Coupled-Channels (CDCC) [10, 11] approach provides a powerful theoretical tool to investigate the fusion-with-breakup process [1–3, 8, 9, 12–17]. By solving the coupled equations, the CDCC method describes the dynamics of the projectile within a complex nuclear potential. However, a comprehensive understanding of the reaction mechanism requires more than calculating the total cross section; it demands a clear explanation of how flux is partitioned and dissipated among different channels. Absorption cross sections are generated by

the imaginary part of the optical potential, and within a coupled-channel framework, this absorption arises not only from diagonal terms but also from the coherent effects of channel-to-channel couplings.

While full-coupling calculations are computationally feasible with modern codes, simplified approaches remain prevalent in recent literature. One common approximation retains off-diagonal couplings within the continuum subspace but neglects couplings between the elastic channel and the continuum ($W_{1j} = 0$ for $j > 1$) [2, 3, 6, 16, 17]; another neglects all off-diagonal imaginary couplings entirely, retaining only diagonal terms [15]. Both approximations effectively assume an incoherent reaction picture in which absorption probabilities add. Such an assumption obscures the cross terms that arise naturally from expanding $\langle \Psi | W | \Psi \rangle$ over channel components. When adopted in the interpretation of experimental data, where model-assisted separations of direct and breakup absorption are common, this approximation can introduce a systematic bias, most notably a systematic underestimation of breakup absorption.

In this work, we rigorously derive a generalized coupled-channel optical theorem within the CDCC framework to address these dynamics. This formalism respects flux conservation in the projected model space and enables the theoretical separation of the total absorption cross section into three physically distinct components: direct absorption (σ_D) from the elastic channel, breakup absorption (σ_B) from the continuum states, and an interference term (σ_{int}) arising from off-diagonal imaginary couplings between the elastic channel and the continuum states. This theoretical separation allows us to go beyond simple incoherent summation and explicitly examine the

* Corresponding author: jinl@tongji.edu.cn

microscopic composition of the absorption process based on the wave functions and coupling potentials.

We emphasize that “coherence” in this work refers specifically to the quantum-mechanical superposition of channel amplitudes during the absorption process: when the total wave function $\Psi = \sum_i \psi_i \phi_i$ is inserted into the absorption functional $\langle \Psi | W | \Psi \rangle$, cross terms $\langle \psi_i | W_{ij} | \psi_j \rangle$ appear alongside diagonal terms. The interference term σ_{int} arising from these cross terms serves as a direct quantitative measure of this coherence. This is distinct from interference between experimentally distinguishable final states, which add incoherently in any measured cross section. Crucially, a non-vanishing σ_{int} constitutes proof that the absorption mechanism involves coherent quantum interference between channels, a physical feature that incoherent summation models fundamentally fail to capture, regardless of the specific numerical value of σ_{int} .

It is important to recognize that while σ_{int} is not directly observable as an asymptotic reaction product, its presence has concrete observable consequences. First, as we demonstrate below, neglecting the off-diagonal couplings that generate σ_{int} produces measurably different elastic scattering angular distributions, an observable quantity that experimentalists can directly test. Second, while the individual values of σ_B and σ_{int} depend on the choice of continuum discretization (bin width, shape, etc.), their sum $\sigma_B + \sigma_{\text{int}}$ is basis-independent and represents the well-defined total continuum contribution to absorption. Thus, experimentalists should care about σ_{int} not for its specific numerical value, but because (i) its existence invalidates incoherent-sum models as a matter of principle, and (ii) theoretical frameworks that neglect it will yield systematically biased extractions of σ_D and σ_B from data. Our numerical results demonstrate that, in the weakly bound systems studied here, σ_{int} is not a negligible perturbative correction but comparable in magnitude to σ_B . Therefore, retaining the full coupling matrix is necessary for the correct physical interpretation of experimental data.

Adopting this perspective of component analysis, we perform a quantitative investigation of reactions induced by deuterons and lithium. Our study focuses on elucidating the dual role of the off-diagonal imaginary couplings in reaction dynamics. We demonstrate that these terms act as a “dynamical bridge,” enhancing flux transfer between the ground state and the continuum, while simultaneously contributing a significant interference term that regulates the overall reaction probability. By analyzing these separated components, we show how the interference mechanism coherently modulates the total absorption and why retaining the full coupling matrix is essential for a precise evaluation of the individual contributions from direct and breakup absorption.

The paper is organized as follows. In Sec. II, we derive the generalized coupled-channel optical theorem and present the decomposition formalism. Section III presents numerical results for $d + {}^{93}\text{Nb}$ and ${}^6\text{Li} + {}^{59}\text{Co}/{}^{208}\text{Pb}$ systems. Finally, Sec. IV summarizes our

findings and discusses their implications.

II. THEORY

A. Derivation of the Coupled-Channel Optical Theorem

To rigorously derive the cross section formulas used in our analysis, we start from the general coupled-channels equations. The system is described by the Hamiltonian $\mathbb{H} = \hat{T}_R + \sum_{i,j} U_{ij}$, leading to the set of coupled equations for the channel wave functions ψ_i :

$$(E_i - \hat{T}_R)\psi_i - \sum_{j=1}^N U_{ij}\psi_j = 0, \quad (1)$$

where \hat{T}_R is the kinetic energy operator and U_{ij} are the coupling potentials.

To simplify the structure and analyze the flux in each channel individually, we introduce the coupled-channels effective optical potential, \bar{U}_i^{cc} , defined by the substitution relation:

$$\bar{U}_i^{cc}\psi_i \equiv \sum_{j=1}^N U_{ij}\psi_j. \quad (2)$$

Substituting Eq. (2) into Eq. (1), the coupled system transforms into a set of formally uncoupled, single-channel equations:

$$(E_i - \hat{T}_R - \bar{U}_i^{cc})\psi_i = 0. \quad (3)$$

This formulation allows us to apply scattering theory techniques to each channel i , distinguishing between the elastic channel (with incident flux) and inelastic channels (without incident flux).

1. Elastic Channel ($i = 1$)

For the elastic channel ($i = 1$), the wave function ψ_1 satisfies the Lippmann-Schwinger integral equation incorporating the incident plane wave ϕ_1 :

$$\psi_1 = \phi_1 + G_0^{(1)} \bar{U}_1^{cc} \psi_1, \quad (4)$$

where $G_0^{(1)} = (E_1 - \hat{T}_R + i\epsilon)^{-1}$ is the free Green’s function. The fundamental optical theorem relates the total cross section σ_T to the imaginary part of the forward scattering amplitude, which is proportional to the transition matrix element $T = \langle \phi_1 | \bar{U}_1^{cc} | \psi_1 \rangle$, the elastic scattering amplitude:

$$f(\theta) = -\frac{\mu}{2\pi\hbar^2} \langle \phi_1(\mathbf{k}') | \bar{U}_1^{cc} | \psi_1(\mathbf{k}) \rangle, \quad (5)$$

where $\mathbf{k}' \cdot \mathbf{k} = k_1^2 \cos \theta$. The optical theorem relates the total cross section, σ_T , to the forward scattering amplitude

$$\begin{aligned}\sigma_T &= \frac{4\pi}{k_1} \text{Im} f(0) \\ &= -\frac{2\mu}{\hbar^2 k_1} \text{Im} \langle \phi_1 | \bar{U}_1^{cc} | \psi_1 \rangle.\end{aligned}\quad (6)$$

To isolate the reaction cross section, we substitute the bra-vector form of Eq. (4), $\langle \phi_1 | = \langle \psi_1 | - \langle \psi_1 | \bar{U}_1^{cc\dagger} G_0^{(1)\dagger}$, into Eq. (6). This decomposes the total cross section into shape elastic (σ_{SE}) and reaction (σ_R) components:

$$\sigma_T = \underbrace{\frac{2\mu}{\hbar^2 k_1} \text{Im} \langle \psi_1 | \bar{U}_1^{cc\dagger} G_0^{(1)\dagger} \bar{U}_1^{cc} | \psi_1 \rangle}_{\sigma_{SE}} - \underbrace{\frac{2\mu}{\hbar^2 k_1} \text{Im} \langle \psi_1 | \bar{U}_1^{cc} | \psi_1 \rangle}_{\sigma_R}. \quad (7)$$

The reaction cross section σ_R is thus generated solely by the expectation value of the imaginary part of the effective potential:

$$\sigma_R = -\frac{2}{\hbar v_1} \text{Im} \langle \psi_1 | \bar{U}_1^{cc} | \psi_1 \rangle. \quad (8)$$

2. Inelastic Channels ($i \neq 1$) and Consistency Proof

For inelastic or breakup channels ($i \neq 1$), there is no incident plane wave ($\phi_i = 0$). The Lippmann-Schwinger equation becomes:

$$\psi_i = G_0^{(i)} \sum_{j=1}^N U_{ij} \psi_j = G_0^{(i)} \bar{U}_i^{cc} \psi_i. \quad (9)$$

The standard definition of the cross section for channel i is the integral of the scattering amplitude squared:

$$\sigma_i = \frac{v_i}{v_1} \int d\Omega_i |f_i(\theta_i)|^2 = \frac{v_i}{v_1} \int d\Omega_i \left| \frac{\mu}{2\pi\hbar^2} \langle \phi_i | \bar{U}_i^{cc} | \psi_i \rangle \right|^2. \quad (10)$$

Alternatively, applying the generalized optical theorem formalism [18], we propose that the cross section can be calculated directly from the effective potential expectation value:

$$\sigma_i = \frac{2}{\hbar v_1} \text{Im} \langle \psi_i | \bar{U}_i^{cc} | \psi_i \rangle. \quad (11)$$

Note the sign difference between Eq. (11) and Eq. (8): the elastic channel carries a minus sign, whereas the inelastic channels do not. This difference reflects the distinct physical content of $\text{Im} \langle \psi_i | \bar{U}_i^{cc} | \psi_i \rangle$ in each case. For the elastic channel ($i = 1$), the effective potential is dominated by the diagonal absorption term U_{11} , whose imaginary part $W_{11} < 0$ removes flux from the incident wave; hence $\text{Im} \langle \psi_1 | \bar{U}_1^{cc} | \psi_1 \rangle < 0$, and a minus sign is required to yield a positive cross section. For

inelastic channels ($i \neq 1$), however, no incident wave exists; the wave function ψ_i is generated entirely by coupling from the elastic channel. The dominant contribution to $\bar{U}_i^{cc} \psi_i = \sum_j U_{ij} \psi_j$ comes from the source term $U_{i1} \psi_1$ rather than the diagonal absorption $U_{ii} \psi_i$, because $|\psi_1| \gg |\psi_i|$. As shown in the proof below, this source-dominated structure leads to $\text{Im} \langle \psi_i | \bar{U}_i^{cc} | \psi_i \rangle > 0$, so no additional sign is needed. *This observation already hints at the central role of ground-state-continuum couplings: neglecting U_{i1} would starve the breakup channels of their primary flux source.*

We now prove that Eq. (11) is consistent with the standard definition in Eq. (10). Starting from the right-hand side of Eq. (11), we substitute the ket-vector ψ_i using the LS equation (Eq. (9)):

$$\text{Im} \langle \psi_i | \bar{U}_i^{cc} | \psi_i \rangle = \text{Im} \langle G_0^{(i)\dagger} \bar{U}_i^{cc} \psi_i | \bar{U}_i^{cc} | \psi_i \rangle = \text{Im} \langle \Phi_i | G_0^{(i)\dagger} | \Phi_i \rangle, \quad (12)$$

where we defined the source term $|\Phi_i\rangle = \bar{U}_i^{cc} |\psi_i\rangle$. Using the operator identity for the Green's function, $\text{Im} G_0^{(i)\dagger} = \pi \delta(E_i - \hat{H}_0)$, and inserting a complete set of plane wave states $\{|\phi_i(\mathbf{k}'_i)\rangle\}$, we obtain:

$$\begin{aligned}\text{Im} \langle \Phi_i | G_0^{(i)\dagger} | \Phi_i \rangle &= \pi \int \frac{d\mathbf{k}'_i}{(2\pi)^3} \langle \Phi_i | \phi_i(\mathbf{k}'_i) \rangle \delta(E_i - E'_i) \langle \phi_i(\mathbf{k}'_i) | \Phi_i \rangle \\ &= \pi \frac{\mu k_i}{(2\pi)^3 \hbar^2} \int d\Omega_i |\langle \phi_i | \bar{U}_i^{cc} | \psi_i \rangle|^2.\end{aligned}\quad (13)$$

Substituting this result back into Eq. (11), the prefactors cancel perfectly to yield:

$$\sigma_i = \frac{2}{\hbar v_1} \left(\pi \frac{\mu k_i}{(2\pi)^3 \hbar^2} \int d\Omega_i |\langle \phi_i | \bar{U}_i^{cc} | \psi_i \rangle|^2 \right) = \frac{v_i}{v_1} \int d\Omega_i |f_i(\theta_i)|^2. \quad (14)$$

This proof confirms that the generalized optical theorem form (Eq. (11)) is mathematically strictly equivalent to the standard cross section definition (Eq. (10)). Beyond its theoretical rigor, this compact formulation is computationally advantageous as it enables the calculation of partial cross sections directly from wave function overlaps, bypassing the need for complex asymptotic integrations.

Physically, this result shows the flux dynamics within inelastic channels ($i \neq 1$), where no incident wave exists. In these channels, σ_i quantifies the net flux emerging from the reaction. It represents the accumulated flux populated by coupling source terms from other channels, accounting for any subsequent reduction caused by the imaginary part of the coupling potential (absorption).

B. Cross Section Analysis within CDCC

We now apply the general formalism derived in Sec. II A to the specific physical problem of projectile breakup. The three-body Hamiltonian describing the collision is

$$\mathbb{H}(\mathbf{R}, \mathbf{r}) = h(\mathbf{r}) + \hat{K}_R + \mathbb{U}^{(1)}(r_1) + \mathbb{U}^{(2)}(r_2), \quad (15)$$

where \mathbf{R} describes the projectile-target relative motion, and \mathbf{r} the projectile internal structure. The fragment-target interactions are complex optical potentials, $\mathbb{U}^{(k)} = V^{(k)} + iW^{(k)}$.

In the Continuum-Discretized Coupled-Channels (CDCC) framework [10, 11, 19], the total wavefunction is expanded in a truncated basis of projectile states $\{\phi_i(\mathbf{r})\}$. This leads to the coupled equations:

$$(E - \epsilon_i - \hat{T}_R) \psi_i(\mathbf{R}) = \sum_{j=1}^N U_{ij}(\mathbf{R}) \psi_j(\mathbf{R}), \quad (16)$$

where the coupling potentials are explicitly defined as:

$$U_{ij}(\mathbf{R}) = \langle \phi_i | \mathbb{U}^{(1)} + \mathbb{U}^{(2)} | \phi_j \rangle = V_{ij}(\mathbf{R}) + iW_{ij}(\mathbf{R}). \quad (17)$$

Here, channel $i = 1$ denotes the elastic channel.

Based on the derived reaction cross section for the elastic channel (Eq. (8)), the total flux loss from the elastic channel, σ_R , is determined by the imaginary part of the couplings connecting to all channels:

$$\begin{aligned} \sigma_R &= -\frac{2}{\hbar v_1} \text{Im} \langle \psi_1 | \bar{U}_1^{cc} | \psi_1 \rangle \\ &= -\frac{2}{\hbar v_1} \text{Im} \left[\sum_{j=1}^N \langle \psi_1 | iW_{1j} | \psi_j \rangle + \sum_{j=2}^N \langle \psi_1 | V_{1j} | \psi_j \rangle \right]. \end{aligned} \quad (18)$$

The flux transferred into the breakup channels (denoted as $i \geq 2$) constitutes the elastic breakup (EBU) cross section. Using the result from the generalized optical theorem for inelastic channels (Eq. (11)), σ_{EBU} is obtained by summing the partial cross sections σ_i :

$$\begin{aligned} \sigma_{\text{EBU}} &= \sum_{i=2}^N \sigma_i = \frac{2}{\hbar v_1} \text{Im} \sum_{i=2}^N \langle \psi_i | \sum_{j=1}^N U_{ij} \psi_j \rangle \\ &= \frac{2}{\hbar v_1} \text{Im} \left[\sum_{i=2}^N \langle \psi_i | V_{i1} | \psi_1 \rangle + \sum_{i=2}^N \langle \psi_i | \sum_{j=1}^N iW_{ij} | \psi_j \rangle \right]. \end{aligned} \quad (19)$$

Within the CDCC framework, elastic scattering and breakup are treated explicitly, while processes such as fusion, transfer, and target excitation are modeled implicitly through the imaginary potentials W_{ij} . The total absorption cross section σ_A quantifies the flux removed by these implicit channels and is defined as the difference between the total reaction cross section and the elastic breakup cross section:

$$\sigma_A = \sigma_R - \sigma_{\text{EBU}}. \quad (20)$$

Substituting Eqs. (18) and (19) into this expression, the terms involving the real coupling potentials V_{ij} cancel out due to the Hermiticity of the potential matrix

($\langle \psi_i | V_{ij} | \psi_j \rangle = \langle \psi_j | V_{ji} | \psi_i \rangle^*$). We are left with the compact result:

$$\begin{aligned} \sigma_A &= -\frac{2}{\hbar v_1} \text{Im} \sum_{i=1}^N \sum_{j=1}^N \langle \psi_i | iW_{ij} | \psi_j \rangle \\ &= -\frac{2}{\hbar v_1} \sum_{i=1}^N \sum_{j=1}^N \langle \psi_i | W_{ij} | \psi_j \rangle. \end{aligned} \quad (21)$$

The second equality follows because the double sum is purely real: for symmetric couplings ($W_{ij} = W_{ji}$), each pair (i, j) and (j, i) contributes $\langle \psi_i | W_{ij} | \psi_j \rangle + \langle \psi_j | W_{ji} | \psi_i \rangle = 2 \text{Re} \langle \psi_i | W_{ij} | \psi_j \rangle$, so the total sum equals its real part.

Equation (21) demonstrates that σ_A is the coherent sum of expectation values of the imaginary coupling potentials. It is important to recognize that the absorption cross section σ_A encompasses *all* flux removed from the CDCC model space by the imaginary potentials. This includes not only complete and incomplete fusion, but also transfer reactions (stripping and pickup) and other non-elastic processes such as deep inelastic scattering. Standard phenomenological optical potentials are fitted to elastic scattering data and do not distinguish among these absorption channels. Consequently, the quantities σ_D (direct) and σ_B (breakup) defined below should be understood as components of the *total absorption*, not exclusively fusion. Isolating specific absorption mechanisms (e.g., fusion vs. transfer) would require either mechanism-specific imaginary potentials or explicit coupling to transfer and other reaction channels, which lies beyond the scope of the present CDCC framework. *Mapping condition:* σ_D and σ_B may be interpreted as proxies for complete and incomplete fusion only when the imaginary potential is specifically designed to represent absorption leading to fusion (e.g., a short-range, strongly absorbing potential localized inside the Coulomb barrier). With standard phenomenological optical potentials, these quantities represent the more general “direct-channel absorption” and “breakup-channel absorption.” Despite this caveat, the central result of this work, that coherent interference generates a significant σ_{int} term, remains valid for any absorption mechanism described by non-diagonal imaginary couplings, including transfer.

To explicitly examine the flux partitioning and the role of quantum interference, we decompose this coherent sum into three physically distinct components:

$$\sigma_A = \sigma_D + \sigma_B + \sigma_{\text{int}}, \quad (22)$$

where σ_D and σ_B represent the diagonal-like absorption from the elastic and continuum channels, respectively.

Basis dependence. We note that while the total absorption σ_A is basis-independent, the partition into σ_D , σ_B , and σ_{int} depends on the choice of channel basis within the continuum subspace. However, two important quantities are basis-independent: (i) σ_D , because the elastic channel (ground state) is uniquely defined by the physical projectile, and (ii) the sum $\sigma_B + \sigma_{\text{int}}$, representing

the total continuum contribution.[20] A unitary rotation among continuum bins redistributes flux between σ_B and σ_{int} individually but leaves their sum invariant. The key physical conclusion, that neglecting W_{1j} modifies both observables (elastic scattering) and the total absorption, is therefore robust under basis changes.

The direct absorption component represents absorption from the elastic channel:

$$\sigma_D = -\frac{2}{\hbar v_1} \langle \psi_1 | W_{11} | \psi_1 \rangle, \quad (23)$$

and the breakup absorption component represents absorption from the continuum states:

$$\sigma_B = -\frac{2}{\hbar v_1} \sum_{i=2}^N \sum_{j=2}^N \langle \psi_i | W_{ij} | \psi_j \rangle. \quad (24)$$

The third term, σ_{int} , represents the interference contribution arising from the off-diagonal imaginary couplings connecting the ground state to the continuum:

$$\sigma_{int} = -\frac{2}{\hbar v_1} \left[\sum_{j=2}^N \langle \psi_1 | W_{1j} | \psi_j \rangle + \sum_{i=2}^N \langle \psi_i | W_{i1} | \psi_1 \rangle \right]. \quad (25)$$

For symmetric couplings ($W_{ij} = W_{ji}$), which hold for fragment-target optical potentials derived from the same nucleon-target interaction, this simplifies to:

$$\sigma_{int} = -\frac{4}{\hbar v_1} \sum_{j=2}^N \text{Re} \langle \psi_1 | W_{1j} | \psi_j \rangle. \quad (26)$$

In both forms, σ_{int} is manifestly real. Its sign depends on the relative phases of the channel wave functions, which are determined by the coupled-channel dynamics.

The decomposition in Eq. (21) highlights that all imaginary parts of the coupling potentials, both diagonal and off-diagonal, contribute coherently to the genuine absorption. If the fragment-target interactions are real ($W^{(1)} = W^{(2)} = 0$), then $\sigma_A = 0$ and $\sigma_R = \sigma_{EBU}$, as expected for pure breakup with no flux loss.

With different models, different imaginary potentials have been used in CDCC calculations of fusion. Hagino et al. [12] and Diaz-Torres and Thompson [8], for example, used the real interaction to generate the coupling potential and utilized a short-range strong-absorption potential on the diagonal term as the fusion process, which is very deep and short-range. This particularly transparent case arises when the imaginary couplings are diagonal in the channel index ($W_{ij} = 0$ for $i \neq j$). In this limit, σ_{int} vanishes, and Eq. (22) reduces to an incoherent sum:

$$\sigma_A = -\frac{2}{\hbar v_1} \sum_{i=1}^N \langle \psi_i | W_{ii} | \psi_i \rangle. \quad (27)$$

The corresponding direct and breakup components are given by Eqs. (23) and (24).

Other CDCC calculations [2, 3, 13, 17] add the fusion potential $W_F^{(k)}$ on the potentials $U^{(k)}$ between the fragments and target:

$$U^{(k)} = V^{(k)} + iW_F^{(k)}. \quad (28)$$

Thus the imaginary part will also appear in the non-diagonal terms in the coupling potentials, which makes it hard to separate the breakup absorption and direct absorption. In many recent studies investigating fusion mechanisms [2, 3, 17], it is common to neglect these off-diagonal imaginary couplings (W_{1j} and W_{j1} , we denote this approximation as $W_{1j} = 0$) between the ground state and continuum states in Eq. (17). Under this approximation, the absorption cross section is simplified to:

$$\sigma_A = \sigma_D + \sigma_B, \quad (29)$$

where $\sigma_D = -\frac{2}{\hbar v_1} \langle \psi_1 | W_{11} | \psi_1 \rangle$ and σ_B is the absorption from continuum states. This model implies that absorption events are localized strictly within individual channels, treating the coupling terms purely as flux transporters with no 'absorption' generated during the transition itself. However, as we demonstrate in the subsequent section, this omission renders the physical description incomplete, as σ_{int} provides a significant coherent contribution to the total absorption.

C. Dynamical polarization potential and a coupling-induced absorption measure

The coupled-channel equations (1) can be rewritten in a single-channel form by introducing the channel-dependent effective (or *polarization*) potential,

$$\bar{U}_i^{cc} \psi_i \equiv \sum_{j=1}^N U_{ij} \psi_j, \quad (30)$$

so that

$$\left(E_i - \hat{T}_R - \bar{U}_i^{cc} \right) \psi_i = 0. \quad (31)$$

For the elastic channel ($i = 1$), it is natural to separate \bar{U}_1^{cc} into the bare elastic potential and an induced term,

$$\bar{U}_1^{cc} = U_{11} + \Delta U_{DPP}, \quad (32)$$

where ΔU_{DPP} is the dynamical polarization potential (DPP) generated by couplings to the breakup (continuum) subspace. In practice, ΔU_{DPP} may be constructed via Feshbach projection [21], or through its trivially equivalent local potential (TELP) [19] representation; the discussion below is independent of the specific construction, as it relies only on the identity (32).

Using the optical-theorem form for the reaction cross section in the elastic channel, Eq. (8), one obtains

$$\sigma_R = -\frac{2}{\hbar v_1} \text{Im} \langle \psi_1 | \bar{U}_1^{cc} | \psi_1 \rangle = \sigma_D + \sigma_{DPP}, \quad (33)$$

with

$$\begin{aligned}\sigma_D &\equiv -\frac{2}{\hbar v_1} \text{Im}\langle\psi_1|U_{11}|\psi_1\rangle, \\ \sigma_{\text{DPP}} &\equiv -\frac{2}{\hbar v_1} \text{Im}\langle\psi_1|\Delta U_{\text{DPP}}|\psi_1\rangle.\end{aligned}\quad (34)$$

Here σ_D represents absorption associated with the bare elastic optical potential, whereas σ_{DPP} isolates the additional reaction flux induced by coupling to the continuum. Therefore, in the present work we use σ_{DPP} as a quantitative measure of the net influence of coupled-channel (continuum) effects on reaction absorption.

The connection between σ_{DPP} and the channel-resolved decomposition in Sec. II B follows from $\sigma_R = \sigma_{\text{EBU}} + \sigma_A$, together with Eq. (22):

$$\sigma_{\text{DPP}} = \sigma_R - \sigma_D = \sigma_{\text{EBU}} + \sigma_A - \sigma_D = \sigma_{\text{EBU}} + \sigma_B + \sigma_{\text{int}}. \quad (35)$$

Equation (35) clarifies the physical content of σ_{DPP} . When the fragment-target interactions are real, $\sigma_A = 0$ and σ_{DPP} reduces to the purely elastic breakup cross section. With complex optical potentials, however, σ_{DPP} contains not only elastic breakup but also continuum-induced absorption, encoded by σ_B and the coherent interference contribution σ_{int} generated by the off-diagonal imaginary couplings. This is precisely why σ_{DPP} provides a convenient and robust diagnostic of coupling effects in our calculations: it quantifies the additional reaction flux attributable to the inclusion of the continuum beyond the bare elastic absorption.

III. RESULTS

A. Role of Off-Diagonal Imaginary Couplings: $d+^{93}\text{Nb}$ Test Case

To quantitatively assess the necessity of retaining the full non-diagonal imaginary coupling matrix W_{ij} , specifically the terms connecting the ground state to continuum bins, we first perform a controlled numerical experiment using the deuteron breakup reaction $d+^{93}\text{Nb}$ at $E_{\text{lab}} = 25.5$ MeV. This system serves as an ideal test case due to its simple two-body cluster structure ($d = p + n$) and manageable model space. We introduce a numerical flag in the CDCC and demonstrate the impact by comparing the full calculation, where all matrix elements $U_{ij} = V_{ij} + iW_{ij}$ are retained, against an approximation where the imaginary couplings between the ground state and continuum are neglected ($W_{1j} = W_{j1} = 0$ for $j \geq 2$, denoted $W_{1j} = 0$ below). In this toy model, we use the same model space: the $p-n$ continuum states are only on $l = 0$ partial wave, using a simple Gaussian interaction as discussed in Ref. [10]. The energy bins are extended to 12 MeV which divided into 6 bin states. The nucleon-target interactions are taken from KD02 [22]. To simplify the calculation, the spins of the particles are ignored, and closed channels are not included in the model space.

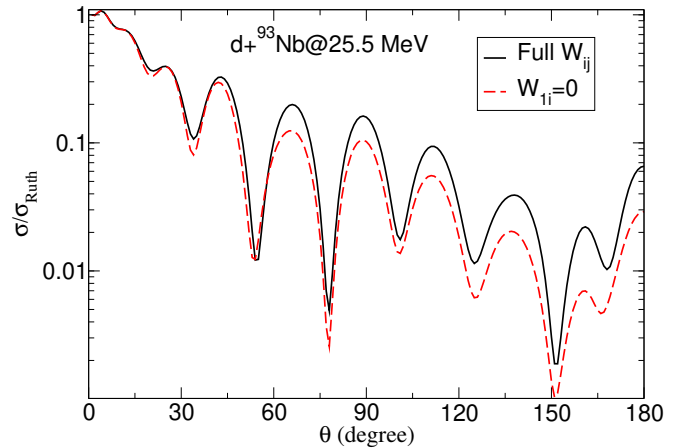


FIG. 1. Elastic scattering cross sections from CDCC calculations (comparing the full calculation and the approximation with $W_{1j} = 0$) for the $d + ^{93}\text{Nb}$ reaction at 25.5 MeV.

Figure 1 presents the elastic scattering cross section distributions from both the full calculation (solid black line) and the approximation with $W_{1j} = 0$ (dashed red line). It is important to note that, even with the relatively simple coupling scheme employed here, significant deviations are observed between the two results, particularly in the intermediate-angle region ($30^\circ - 120^\circ$). These differences are not merely quantitative; they reflect fundamentally different scattering dynamics.

In the full calculation, the off-diagonal imaginary couplings W_{1j} (coupling the elastic channel to continuum bins) allow coherent flux redistribution through quantum interference effects. When these couplings are artificially set to zero, the scattering amplitude loses this interference mechanism, resulting in a systematically different angular distribution. The most striking differences occur around $\theta \approx 60^\circ$ and 120° , where the full calculation exhibits deeper minima compared to the approximation. This leads to a crucial observation: although σ_{int} itself is not an asymptotic observable, neglecting it produces measurable consequences in the elastic channel. Any theoretical framework that omits the off-diagonal imaginary couplings will fail to reproduce the correct elastic angular distribution, providing experimentalists with a direct, testable criterion for the necessity of retaining the full coupling matrix.

To facilitate the discussion of flux dynamics, we analyze the calculated absorption cross sections using the coherent decomposition defined in Eq. (22). As shown in Table I, the interference term σ_{int} represents the coupling effect between the elastic and continuum channels. When the ground-state-to-continuum imaginary couplings are artificially neglected, σ_{int} vanishes by definition, and the total absorption reduces to the incoherent sum (Eq. (29)).

The comparison of absorption cross-section matrices, shown in Figure 2, reveals that the interference terms in the full calculation exhibit significant negative values. As derived in Eq. (21), these negative contributions

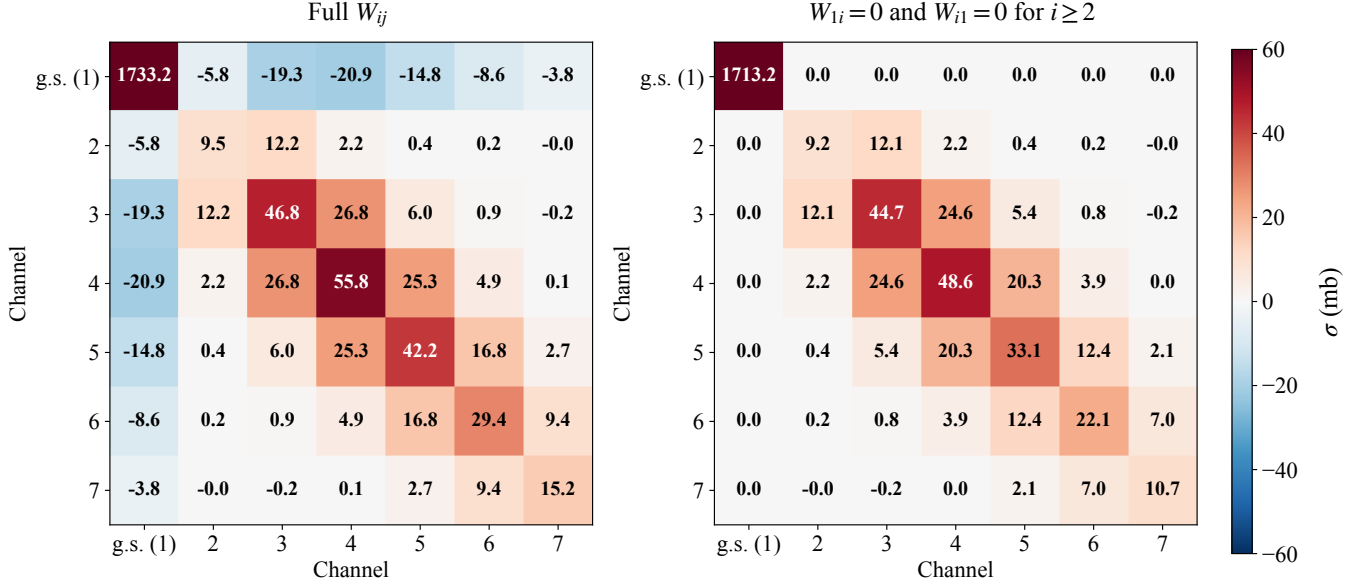


FIG. 2. Comparison of absorption cross-section matrices for $d+^{93}\text{Nb}$ at 25.5 MeV ($l = 0$ bins). **Left:** Full coupling calculation. **Right:** Approximation with $W_{1j} = 0$. The negative off-diagonal values in the full calculation (left) indicate coherent interference flux loss, which is artificially removed in the approximation (right).

TABLE I. Impact of neglecting W_{1j} on absorption cross sections for $d+^{93}\text{Nb}$ ($l = 0$ bins). The "Diff." column represents $(\text{Full } W_{ij} - W_{1j} = 0)$.

Quantity	Full W_{ij}	$W_{1j} = 0$	Diff.
σ_D [mb]	1733.2	1713.2	+20.0
σ_B [mb]	414.1	350.8	+63.3
σ_{int} [mb]	-146.7	0.0	-146.7
σ_A [mb]	2000.7	2064.0	-63.3

in the off-diagonal blocks are a direct signature of the quantum interference between the elastic and continuum channels. Table I summarizes the quantitative impact of neglecting these terms. In the full calculation, the interference term is substantial and negative ($\sigma_{\text{int}} = -146.7$ mb), which acts to reduce the total absorption cross section via destructive interference. When we artificially set $\sigma_{\text{int}} = 0$ in the approximation, the flux distribution is fundamentally altered. Contrary to naive expectations, the total absorption cross section in the approximation ($\sigma_A = 2064.0$ mb) is actually larger than in the full calculation ($\sigma_A = 2000.7$ mb). This counterintuitive result occurs because the approximation removes the large negative interference term that naturally regulates the total absorption in the full physical picture. Simultaneously, the removal of the coupling leads to a significant underestimation of the breakup absorption component, with σ_B dropping from 414.1 mb to 350.8 mb, and a slight decrease in direct absorption σ_D from 1733.2 mb to 1713.2 mb.

This comparison demonstrates that absorption in-

volves a coherent superposition where the interference couplings play a dual role: they serve to enhance the specific absorption pathways (σ_B and σ_D) by redistributing flux between channels, while simultaneously reducing the total reaction probability through destructive interference. Consequently, the approximation of neglecting off-diagonal imaginary couplings fails on two fronts: it overestimates the total absorption while underestimating the individual absorption components. This implies that prior analyses based on incoherent approximations likely underestimated breakup absorption cross sections. As noted in Sec. II B, the specific numerical partition between σ_B and σ_{int} is basis-dependent, but their sum $\sigma_B + \sigma_{\text{int}}$ (the total continuum contribution) and the qualitative conclusions regarding coherent interference remain basis-independent.

B. Absorption Mechanism in Weakly Bound Nuclei: ${}^6\text{Li}$ Case

Building on the insights from the deuteron case, we turn our attention to the heavier and more complex projectile, ${}^6\text{Li}$, examining the ${}^6\text{Li}+{}^{59}\text{Co}$ reaction at 21.5 MeV and the ${}^6\text{Li}+{}^{208}\text{Pb}$ reaction at 33 MeV. The ${}^6\text{Li}$ projectile is modeled with an $\alpha - d$ cluster structure, including continuum states up to partial waves $\ell \leq 1$. The continuum is discretized up to excitation energies of 16 MeV (for ${}^{59}\text{Co}$) and 20 MeV (for ${}^{208}\text{Pb}$). This expanded model space allows us to probe the interference effects in a system with more degrees of freedom than the deuteron.

Numerical robustness. To ensure that the qualitative conclusions are not artifacts of discretization, we have

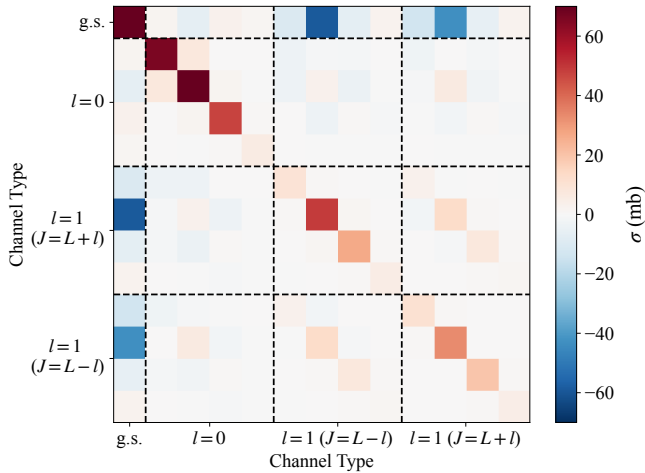


FIG. 3. Decomposition of the total absorption cross section σ_A for ${}^6\text{Li} + {}^{59}\text{Co}$ at 21.5 MeV. Red indicates positive contributions, while blue indicates negative contributions.

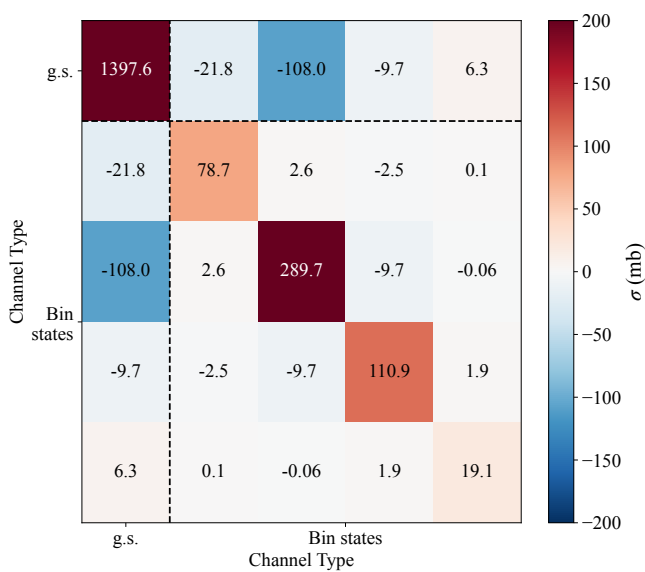


FIG. 4. Decomposition in the different bin energies of the total absorption cross section σ_A for ${}^6\text{Li} + {}^{59}\text{Co}$ at 21.5 MeV. Red indicates positive contributions, while blue indicates negative contributions.

verified convergence with respect to the key model-space parameters: number of bins, maximum excitation energy, maximum partial wave ℓ_{\max} , and integration parameters (matching radius R_{\max} and radial step size). Varying the number of bins by $\pm 20\%$ or extending E_{\max} by 4 MeV changes σ_A by less than 3% and leaves the ratio $\sigma_{\text{int}}/\sigma_A$ stable to within 10%. The pattern of large negative σ_{int} and enhanced component cross sections in the full calculation persists across all tested discretization schemes, confirming that these are robust physical features rather than numerical artifacts.

Figure 3 visualizes the absorption cross-section decom-

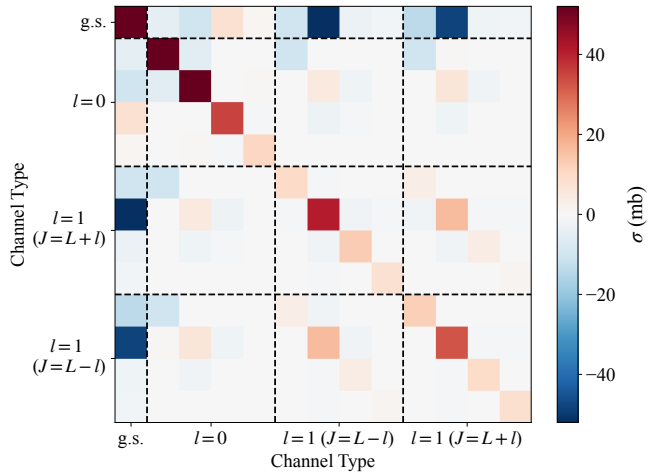


FIG. 5. Decomposition of the total absorption cross section σ_A for ${}^6\text{Li} + {}^{208}\text{Pb}$ at 33 MeV.

position for the ${}^6\text{Li} + {}^{59}\text{Co}$ system. The heatmap reveals a distinct topological structure: the diagonal elements (red) representing direct absorption (σ_D) and breakup absorption (σ_B) are universally positive, whereas the off-diagonal elements (blue) representing the interference term (σ_{int}) are predominantly negative. This pattern is particularly pronounced for the $l = 1$ continuum states. Physically, the $l = 1$ (p -wave) continuum in ${}^6\text{Li}$ corresponds to the α - d relative motion with one unit of angular momentum, which couples strongly to the $l = 0$ ground state through the dipole component of the fragment-target interaction. This strong coupling, combined with the lower centrifugal barrier for $l = 1$ compared to higher partial waves, produces large off-diagonal matrix elements W_{1j} and hence dominant interference contributions. The energy-resolved perspective in Fig. 4 further confirms that this interference is not an artifact of energy averaging; rather, the negative σ_{int} contribution persists across the excitation energy spectrum, actively competing with the positive breakup absorption terms. A qualitatively similar pattern is observed for the heavier target system, ${}^6\text{Li} + {}^{208}\text{Pb}$ (Figure 5), indicating that this interference mechanism is a robust feature of weakly bound projectile reactions, independent of the target mass.

To quantify the dynamical role of the ground state-continuum couplings, we demonstrate the impact by comparing the full calculation with the approximation ($W_{1j} = 0$) in Table II. The results reveal a profound flux redistribution mechanism that is consistent between the Co and Pb targets but far more dramatic in magnitude than the deuteron case. In the full calculation, the interference term σ_{int} provides a massive negative contribution (-266.7 mb for Co and -283.8 mb for Pb), which acts to regulate the total absorption cross section. Consequently, neglecting these terms in the approximation leads to an overestimation of the total cross section (σ_A) by approximately 5% for Co and 10% for Pb.

However, the most striking physical insight lies in the

TABLE II. Impact of neglecting W_{1j} on absorption cross sections for the ${}^6\text{Li}$ system.

Quantity	Full W_{ij}	$W_{1j} = 0$	Diff.
${}^6\text{Li} + {}^{59}\text{Co}$ @ 21.5 MeV			
σ_D [mb]	1397.6	1335.9	+61.7
σ_B [mb]	483.4	356.0	+127.4
σ_{int} [mb]	-266.7	0.0	-266.7
σ_A [mb]	1614.4	1691.9	-77.5
${}^6\text{Li} + {}^{208}\text{Pb}$ @ 33 MeV			
σ_D [mb]	1030.3	990.3	+40.0
σ_B [mb]	299.9	164.8	+135.1
σ_{int} [mb]	-283.8	0.0	-283.8
σ_A [mb]	1046.4	1155.0	-108.6

decomposition of the absorption components. The full calculation shows significantly higher values for both direct absorption (σ_D) and breakup absorption (σ_B) compared to the approximation. For the ${}^6\text{Li} + {}^{59}\text{Co}$ system, the full coupling enhances σ_B by 127.4 mb (from 356.0 to 483.4 mb). This enhancement is even more critical in the ${}^6\text{Li} + {}^{208}\text{Pb}$ system, where σ_B nearly doubles, increasing by 135.1 mb (from 164.8 to 299.9 mb). This implies that the off-diagonal imaginary couplings act as a "pump," facilitating the transfer of flux from the elastic channel into the breakup absorption channels. When W_{1j} is removed, this bridge is broken, starving the breakup absorption channels of flux.

These findings challenge the validity of incoherent approximations for weakly bound nuclei. The interference couplings play a dual role: they enhance specific reaction pathways (boosting σ_D and σ_B), while simultaneously contributing a negative interference term that reduces the total reaction probability. Thus, retaining the full non-diagonal imaginary coupling matrix is necessary for correctly predicting the partitioning of flux between direct and breakup mechanisms.

IV. SUMMARY AND DISCUSSION

In this work, we have presented a rigorous derivation of the generalized optical theorem within the Continuum-Discretized Coupled-Channels (CDCC) framework and investigated the role of off-diagonal imaginary couplings in the absorption mechanism of weakly bound nuclei. By decomposing the total absorption cross section into direct absorption (σ_D), breakup absorption (σ_B), and the interference term (σ_{int}), we have elucidated the complex quantum interference effects that govern the redistribution of reaction flux.

The theoretical analysis establishes that the total absorption is not merely an incoherent sum of channel probabilities. Instead, it includes coherent interference terms (σ_{int}) arising from the off-diagonal imaginary couplings (W_{ij}). Our numerical calculations for $d + {}^{93}\text{Nb}$

and ${}^6\text{Li} + {}^{59}\text{Co}/{}^{208}\text{Pb}$ consistently demonstrate that these interference terms are predominantly negative in the systems studied, representing a destructive interference mechanism that plays a central role in flux conservation within the model space.

The comparison between full coupled-channel calculations and approximations neglecting ground state-continuum couplings ($W_{1j} = 0$) reveals a dual and contradictory dynamical role played by the interference terms: The off-diagonal imaginary couplings act as a dynamical bridge, facilitating the transfer of flux from the elastic channel to the continuum and back. This "pumping" effect significantly enhances the specific absorption pathways. As observed in the ${}^6\text{Li}$ cases, retaining the full coupling matrix increases the breakup absorption cross section (σ_B) by approximately 35% for the Co target and nearly doubles it (an 82% increase) for the Pb target. Direct absorption (σ_D) is similarly reinforced.

Simultaneously, in all the systems and energy ranges examined here, σ_{int} is found to be large and negative, ensuring that this enhanced internal flux does not violate conservation laws. It acts as a regulator, reducing the total reaction probability via destructive interference. We note that the sign of σ_{int} is an empirical observation from our numerical calculations; a general proof that destructive interference must occur in weakly bound systems remains an open question for future theoretical investigation. Consequently, neglecting these terms leads to the counterintuitive result where the total absorption cross section is overestimated, while the individual absorption components are significantly underestimated.

This analysis clarifies why simplified models that neglect off-diagonal imaginary couplings yield a physically incomplete picture.

A potential objection is that the comparison between full and $W_{1j} = 0$ calculations in this work employs identical optical potential parameters. One might argue that re-fitting the parameters within the $W_{1j} = 0$ approximation could restore agreement with elastic scattering data, effectively "renormalizing" the missing σ_{int} physics into adjusted potential depths or geometries. While such parameter adjustment may indeed recover acceptable fits to elastic angular distributions, it comes at the cost of distorting the extracted component cross sections. The re-fitted parameters would compensate for the missing coherent interference by artificially modifying the absorption strengths, leading to systematically biased values of σ_D and σ_B . This is precisely the core message of the present work: merely reproducing experimental observables is insufficient; the underlying reaction mechanism must be correctly captured. A model that fits data through parameter tuning but misrepresents the flux partitioning will yield misleading physical interpretations, particularly when extrapolating to unmeasured observables or different reaction systems.

Direct experimental validation of individual components, and specifically the interference term σ_{int} , is intrinsically impossible: detectors register asymptotic

products, not internal coherence terms of the wave function. Component extractions (*e.g.*, direct vs. breakup fractions) are therefore model-dependent. Moreover, we emphasize that the absorption cross section σ_A calculated within the CDCC framework includes all flux absorbed by the imaginary potentials, encompassing not only fusion but also transfer reactions, deep inelastic scattering, and other non-elastic channels. The quantities σ_D and σ_B should be interpreted as components of total absorption rather than pure fusion. Disentangling genuine fusion from transfer would require either fusion-specific short-range potentials or explicit coupling to transfer channels. Nevertheless, the central conclusion, that coherent interference generates a significant σ_{int} term (observed to be negative in the systems studied), applies to any absorption mechanism governed by non-diagonal imaginary couplings. The value of the present work is to provide a rigorous theoretical constraint (the generalized optical theorem and its component analysis) based on flux conservation.

Implications for experimental analysis. Our findings have direct consequences for the extraction of reaction cross sections from experimental data. A common experimental procedure is to measure the total fusion cross section and then use theoretical models to partition it into complete fusion (direct) and incomplete fusion (breakup-induced) components. If the theoretical model employed for this partition neglects the off-diagonal imaginary couplings, as is done in many simplified CDCC or optical model analyses, the extracted breakup contribution will be systematically underestimated. We therefore urge experimentalists to adopt full-coupling CDCC calculations, retaining all W_{ij} terms, as the baseline for any model-

assisted decomposition of absorption data (which may be identified with fusion when the imaginary potential is designed specifically for fusion absorption). Furthermore, when comparing theoretical predictions with measured elastic scattering angular distributions, the full-coupling calculation should be used; as shown in Fig. 1, simplified models produce qualitatively different angular distributions that could lead to incorrect conclusions about the adequacy of the optical potential parametrization.

In conclusion, the component analysis presented here demonstrates that accurate predictions for weakly bound nuclei require the retention of the full non-diagonal imaginary coupling matrix. The quantum interference mediated by these couplings is not merely a perturbative correction but a significant driver of reaction dynamics in the systems studied. It determines the correct partitioning between direct and breakup mechanisms while respecting flux conservation, providing a robust framework for future studies of complex fusion dynamics. Beyond CDCC, the generalized optical-theorem-based component analysis is applicable to broader coupled-channel problems (including transfer), and we advocate it as a standard paradigm for mechanism-resolved extraction of reaction observables.

ACKNOWLEDGMENTS

We thank Antonio M. Moro for useful discussions. This work was supported by the National Natural Science Foundation of China (Grant Nos. 12535009 and 12475132), the National Key R&D Program of China (Contract No. 2023YFA1606503), and the Fundamental Research Funds for the Central Universities.

[1] A. Diaz-Torres, D. J. Hinde, J. A. Tostevin, M. Dasgupta, and L. R. Gasques, *Phys. Rev. Lett.* **98**, 152701 (2007).

[2] G. D. Kolinger, L. F. Canto, R. Donangelo, and S. R. Souza, *Phys. Rev. C* **98**, 044604 (2018).

[3] M. R. Cortes, J. Rangel, J. L. Ferreira, J. Lubian, and L. F. Canto, *Phys. Rev. C* **102**, 064628 (2020).

[4] J. Lei and A. M. Moro, *Phys. Rev. Lett.* **123**, 232501 (2019).

[5] E. Takada, T. Shimoda, N. Takahashi, T. Yamaya, K. Nagatani, T. Udagawa, and T. Tamura, *Phys. Rev. C* **23**, 772 (1981).

[6] J. Rangel, B. Pinheiro, V. A. B. Zagatto, J. Lubian, F. M. Nunes, and L. F. Canto, “Nucleus-nucleus potentials in the scattering of tightly and weakly bound systems,” (2025), arXiv:2507.11050 [nucl-th].

[7] N. Takigawa, M. Kuratani, and H. Sagawa, *Phys. Rev. C* **47**, R2470 (1993).

[8] A. Diaz-Torres and I. J. Thompson, *Phys. Rev. C* **65**, 024606 (2002).

[9] L. Canto, P. Gomes, R. Donangelo, J. Lubian, and M. Hussein, *Physics Reports* **596**, 1 (2015), recent developments in fusion and direct reactions with weakly bound nuclei.

[10] N. Austern, Y. Iseri, M. Kamimura, M. Kawai, G. Rawitscher, and M. Yahiro, *Physics Reports* **154**, 125 (1987).

[11] J. Lei and A. M. Moro, *Phys. Rev. C* **108**, 034612 (2023).

[12] K. Hagino, A. Vitturi, C. H. Dasso, and S. M. Lenzi, *Phys. Rev. C* **61**, 037602 (2000).

[13] P. Descouvemont, T. Druet, L. F. Canto, and M. S. Hussein, *Phys. Rev. C* **91**, 024606 (2015).

[14] N. Keeley, K. Kemper, and K. Rusek, *Phys. Rev. C* **65**, 014601 (2001).

[15] A. Diaz-Torres, I. J. Thompson, and C. Beck, *Phys. Rev. C* **68**, 044607 (2003).

[16] J. Rangel, M. Cortes, J. Lubian, and L. Canto, *Physics Letters B* **803**, 135337 (2020).

[17] J. Lubian, J. L. Ferreira, J. Rangel, M. R. Cortes, and L. F. Canto, *Phys. Rev. C* **105**, 054601 (2022).

[18] S. R. Cotanch, *Nuclear Physics A* **842**, 48 (2010).

[19] I. J. Thompson and F. M. Nunes, *Nuclear Reactions for Astrophysics: Principles, Calculation and Applications of Low-Energy Reactions* (Cambridge University Press, 2009).

[20] To see this, let P_g project onto the ground state and $P_c = 1 - P_g$ onto the continuum subspace. Then $\sigma_A \propto$

$-\langle \Psi | W | \Psi \rangle$ and $\sigma_D \propto -\langle \Psi | P_g W P_g | \Psi \rangle$. The remainder, $\sigma_A - \sigma_D \propto -\langle \Psi | (P_c W P_c + P_g W P_c + P_c W P_g) | \Psi \rangle$, is invariant under any unitary transformation U acting within the continuum subspace ($P_c \rightarrow U P_c U^\dagger$), since both the basis states and the operator transform together, leaving the expectation value unchanged.

- [21] H. Liu, J. Lei, and Z. Ren, “Exact treatment of continuum couplings in nuclear optical potentials via feshbach theory,” (2025), [arXiv:2508.07584 \[nucl-th\]](https://arxiv.org/abs/2508.07584).
- [22] A. Koning and J. Delaroche, *Nuclear Physics A* **713**, 231 (2003).